

# Integration of fiber coupled high- $Q$ $\text{SiN}_x$ microdisks with magnetostatic atom chips

Paul E. Barclay,\* Kartik Srinivasan, and Oskar Painter  
Thomas J. Watson, Sr. Laboratory of Applied Physics,  
California Institute of Technology, Pasadena, CA 91125, USA.

Benjamin Lev and Hideo Mabuchi  
Norman Bridge Laboratory of Physics, California Institute of Technology, Pasadena, CA 91125, USA.  
(Dated: May 29, 2006)

Micron scale silicon nitride microdisk optical resonators fabricated on a silicon wafer are demonstrated with  $Q = 3.6 \times 10^6$  (finesse =  $5 \times 10^4$ ) and an effective mode volume of  $15(\lambda/n)^3$  at wavelengths  $\lambda \sim 852$  nm resonant with the D2 transition manifold of cesium. A dilute hydrofluoric wet etch is shown to provide sensitive tuning of the microdisk optical resonances, and robust mounting of a fiber taper provides efficient fiber optic coupling to the  $\text{SiN}_x$  microdisk cavities while allowing unfettered optical access for laser cooling and trapping of atoms. Initial measurement of a hybrid atom-cavity chip indicates that cesium adsorption on the surface of the  $\text{SiN}_x$  microdisks results in significant red-detuning of the disk resonances. A technique for parallel integration of multiple (10) microdisks with a single optical fiber taper is also demonstrated.

PACS numbers:

Atom chip technology[1, 2] has rapidly evolved over the last decade as a valuable tool in experiments involving the cooling, trapping, and transport of ultra-cold neutral atom clouds. During the same period there has been significant advancement in microphotonic systems[3] for the guiding and trapping of light in small volumes, with demonstrations of photonic crystal nanocavities capable of efficiently trapping light within a cubic wavelength[4] and chip-based silica microtoroid resonators[5] with photon lifetimes well over  $10^8$  optical cycles. Poised to significantly benefit from these developments is the field of cavity quantum electrodynamics (cavity QED)[6], in which strong interactions of atoms with light inside a resonant cavity can be used to aid in quantum information processing and in the communication and distribution of quantum information within a quantum network[7]. Integration of atomic and microphotonic chips[8, 9, 10] offers several advancements to the current state-of-the-art Fabry-Perot cavity QED systems[11], most notably a scalable platform for locally controlling multiple quantum bits and an increased bandwidth of operation. In this Letter we demonstrate the suitability of silicon nitride ( $\text{SiN}_x$ ) for high- $Q$ , small mode volume microcavities resonant at near-visible wavelengths necessary for cavity QED with alkali atoms, and describe a robust mounting technique which enables the integration of a permanently fiber-coupled microdisk resonator with a magnetostatic atom chip.

In addition to the obvious benefits of the fabrication maturity of the silicon(Si)-silicon oxide( $\text{SiO}_x$ ) materials system, recent work has shown that high quality atom chips can be created from thermally evaporated gold metal wires on thin oxide coated Si wafers[12]. Integration with a  $\text{SiN}_x$  optical layer provides a path towards a monolithic atom-cavity chip with integrated atomic and photonic functionality. Indeed, owing to its moderately high index of refraction ( $n \sim 2.0$ - $2.5$ ) and large transparency window ( $6 \mu\text{m} > \lambda > 300$  nm)[13, 14],  $\text{SiN}_x$  is an excellent material for the on-chip guiding and localization

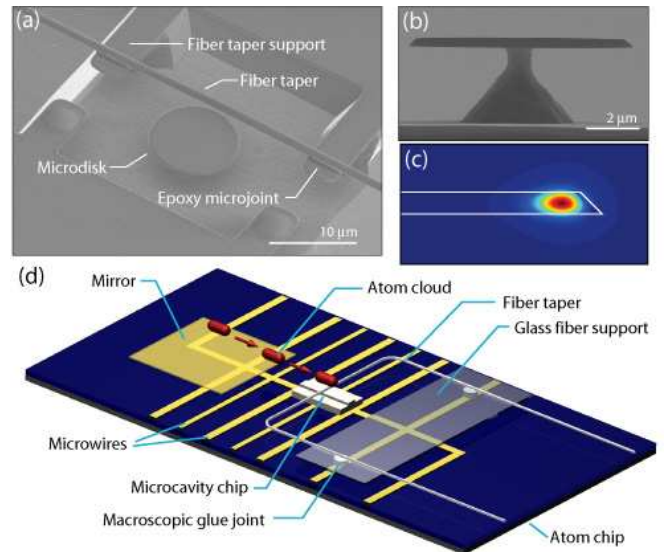


FIG. 1: (a) Scanning electron microscope (SEM) image of a  $\text{SiN}_x$  cavity coupled to an optical fiber taper. The fiber taper is permanently aligned a few hundred nanometers from the microdisk circumference with epoxy microjoints to  $\text{SiN}_x$  supports. (b) Side-view SEM image of a  $9 \mu\text{m}$  diameter microdisk. (c) FEM calculated field distribution ( $|E|^2$ ) of a  $m = 50, p = 1$ , TE-like mode of the microdisk in (b). (d) Schematic of the integrated atom-cavity chip.

of light. The high refractive index of  $\text{SiN}_x$  makes possible the creation of a variety of wavelength scale microcavity geometries such as whispering-gallery [15, 16] or planar photonic crystal structures[17], with a small intrinsic radiation loss. Combined with a lower index  $\text{SiO}_x$  cladding, waveguiding in a  $\text{SiN}_x$  layer can be used to distribute light within a planar microphotonic circuit suitable for high-density integration. The low absorption loss across the visible and near-IR wavelengths, on the other hand, allows  $\text{SiN}_x$  to be used

with a diverse set of atomic and atomic-like (colloidal quantum dots, color centers, etc.) species. Beyond the particular focus of this work on cavity QED experiments with cold alkali atoms, high- $Q$  SiN<sub>x</sub> microcavities are also well suited to experiments involving moderate refractive index environments, such as sensitive detection of analytes contained in a fluid solution[18, 19] or absorbed into a low index polymer cladding[20].

The SiN<sub>x</sub> microdisk resonators in this work were fabricated from a commercially available Si wafer with a 250 nm thick stoichiometric SiN<sub>x</sub> ( $n = 2.0$ ) layer grown on the surface by low pressure chemical vapor deposition (LPCVD). Fabrication of the microdisk resonators involved several steps, beginning with the creation of a highly circular electron beam resist etch mask through electron beam lithography and a resist reflow[21]. A C<sub>4</sub>F<sub>8</sub>/SF<sub>6</sub> plasma dry etch was optimized to transfer the resist etch mask into the SiN<sub>x</sub> layer as smoothly as possible. This was followed by a potassium hydroxide wet etch to selectively remove the underlying  $\langle 100 \rangle$  Si substrate until the SiN<sub>x</sub> microdisks were supported by a small micron diameter silicon pillar. A final cleaning step to remove organic materials from the disk surface was performed using a H<sub>2</sub>SO<sub>4</sub>:H<sub>2</sub>O<sub>2</sub> wet etch. A SEM image of a fully processed microdisk is shown in Fig 1(a,b).

The optical modes of the fabricated microdisks were efficiently excited via an optical fiber taper waveguide[22, 23]. A swept wavelength source covering the 840-856 nm wavelength band was coupled into the fiber taper waveguide and used to measure the fine transmission spectra of the microdisk resonators at wavelengths close to the D2 transition of cesium (Cs). Details of the fiber taper measurement set-up can be found in Ref. 21. Figure 2(a) shows a typical measured wavelength scan of the lowest radial order ( $p = 1$ ) TE-like mode of a 9  $\mu\text{m}$  diameter SiN<sub>x</sub> microdisk. The resonance has an intrinsic linewidth of 0.26 pm, corresponding to a quality factor  $Q = 3.6 \times 10^6$ . The doublet structure in the transmission spectra is due to mode-coupling between the clockwise and counter-clockwise modes of the disk due to surface roughness induced backscattering[24]. In addition to this high- $Q$  mode, the 9  $\mu\text{m}$  microdisks also support a lower  $Q$  higher-order radial mode in the 850 nm wavelength band. The free spectral range between modes of the same radial order but different azimuthal number ( $m$ ) was also measurable, and found to be 5.44 THz (13 nm) for these small microdisks. The resulting finesse of these cavities is  $\mathcal{F} = 5 \times 10^4$ . Tests of less surface sensitive larger diameter microdisks showed reduced doublet splitting but no reduction in linewidth, indicating that  $Q$  is most likely limited by intrinsic material absorption[21].

Finite-element method (FEM) simulations[21] (Fig. 1(c)) show that the effective optical mode volume, defined by  $V_{\text{eff}} = \int n^2(\mathbf{r})E^2(\mathbf{r})d\mathbf{r} / n^2(\mathbf{r})E^2(\mathbf{r})|_{\text{max}}$ , is as small as 15  $(\lambda/n)^3$  for the 9  $\mu\text{m}$  diameter microdisks. The corresponding parameters of cavity QED, the Cs-photon coherent coupling rate ( $g$ ), photon decay rate ( $\kappa$ ), and Cs transverse decay rate ( $\gamma_{\perp}$ ) are  $[g, \kappa, \gamma_{\perp}] / 2\pi = [1.3, 0.05, 0.003]$  GHz, indicating that these SiN<sub>x</sub> microdisk cavities are capable of operating well

within the regime of strong coupling[6]. Here an FEM calculated value of  $\eta \sim 0.3$  was used to relate the electric field strength at the SiN<sub>x</sub> disk surface that a Cs atom might experience to the actual maxima inside the disk. Although much smaller microdisks can be fabricated, FEM simulations show that the intrinsic radiation  $Q$  drops rapidly below the  $10^8$  level as the diameter becomes smaller than 9  $\mu\text{m}$ .

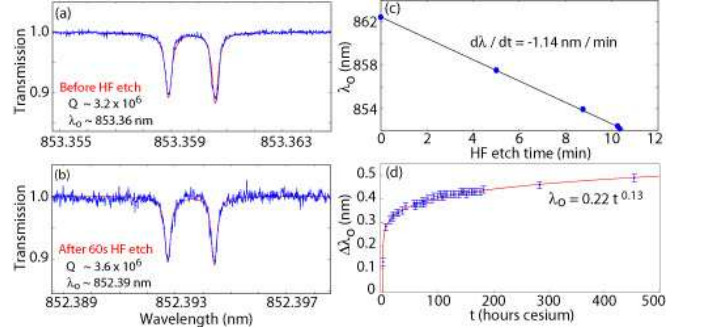


FIG. 2: (a) Wavelength scan of the fiber taper transmission for a  $p = 1$  TE-like mode of a 9  $\mu\text{m}$  diameter SiN<sub>x</sub> microdisk, prior to HF etch tuning, and (b) after HF wet etch tuning of the resonance wavelength showing no degradation in  $Q$ . (c) Resonance wavelength ( $\lambda_o$ ) of the  $p = 1$  TE-like mode of an 11  $\mu\text{m}$  diameter microdisk as a function of HF etch time. The wet etch was interrupted at the time of each data point for the measurement of  $\lambda_o$ . (d) Shift in the  $p = 1$  TE-like resonance wavelength as a function of time exposed to cesium vapor (partial pressure  $\sim 10^{-9}$  Torr) in a UHV chamber.

Using the fabrication procedure described above, the resonance wavelength of the microdisk modes could be positioned with an accuracy of roughly one part in a thousand, corresponding to variations in the average disk radius of about 10 nm from disk-to-disk. In order to finely tune the resonance wavelength ( $\lambda_o$ ) into alignment with the D2 atomic Cs transition a series of timed etches in 20:1 diluted 49% HF solution were employed. By slowly etching the LPCVD SiN<sub>x</sub> the resonance wavelength of the high- $Q$  disk modes was shown to blue shift at a rate of 1.1 nm/min (Fig. 2(c)). With this technique the cavity resonance could be positioned with an accuracy of  $\pm 0.05$  nm without degrading the  $Q$  factor (Fig. 2(b)). Further fine tuning can be accomplished by heating and cooling of the sample; a temperature dependence of  $d\lambda_o/dT \sim 0.012$  nm/ $^{\circ}\text{C}$  was measured for the  $p = 1$ , TE-like microdisk modes.

After initial device characterization and tuning of  $\lambda_o$ , a fiber taper and microdisk chip were integrated with an atom chip. A brief outline of the integration procedure follows. The microcavity chip is first aligned and then bonded to the desired location on the atom chip using polymethyl methacrylate. The fiber taper is supported in a self-tensioning “U” configuration [25] by a glass coverslip ( $\sim 200$   $\mu\text{m}$  thickness), as illustrated in Fig. 1(d). The taper is aligned with the microdisk using a three-axis DC stepper motor stage with 50 nm encoder resolution. Adjustment in the lateral gap between the taper and the microdisk is used to obtain the desired level of cavity loading; owing to the excellent phase matching of the fiber taper guided

mode to the whispering-gallery modes of the microdisk[26] critical coupling was possible with a loaded  $Q \sim 10^6$ . The fiber taper and microdisk are then permanently attached using UV curable epoxy (supplied by Dymax) in two regions: (i) microscopic glue joints between the fiber taper and lithographically defined  $\text{SiN}_x$  supports, shown in Fig. 1(a), fix the position of the taper relative to the disk; (ii) macroscopic glue joints between the taper support slide and the atom chip, as schematically shown in Fig. 1(d), fix the position of the taper support relative to the chip and serve as stress relief points for the fiber pigtailed. The entire fiber taper mount must lie below the plane of the optically trapped and magnetically guided atoms ( $\sim 600 \mu\text{m}$ ). A sufficiently low-profile is achieved by aligning and bonding the taper support glass coverslip parallel to and below the plane of the microdisk chip top surface. During the taper mounting procedure the taper-microdisk coupling is monitored by measuring the resonance wavelength and transmission contrast, with no noticeable change being observed during the curing of the epoxy joints. The micro glue joints incur a taper diameter dependent amount of broadband insertion loss; for the taper diameters used here ( $\sim 1 \mu\text{m}$ ) an approximate 10-15% optical loss per joint is typical. Post-cure, the fiber-cavity alignment is extremely robust, withstanding all of the vacuum installation procedures described below.

The integrated atom-cavity chip was installed in an ultra-high vacuum (UHV) chamber designed for performing atom chip waveguiding experiments. Vacuum-safe fiber feedthroughs were fabricated from teflon inserts within a swagelock compression fitting[27] and used to pass the fiber-pigtails out of the chamber. The chamber was evacuated using turbo and ion pumps and baked at  $130 \text{ }^\circ\text{C}$  for 24 hours so that a background pressure of  $\sim 10^{-8}$  Torr was reached. Initial experiments with the integrated system involved the trapping of Cs atoms in a mirror-MOT[1] above the gold mirror region in the illustration of Fig. 1(d), and transfer of atoms to a micro-U-MOT [1] just above the mirror surface using microwire currents on the atom chip. The extremely low-profile of the fiber taper mounting was shown to provide excellent optical access for atom trapping, cooling, and imaging. The microdisk resonance wavelength and transmission contrast were continuously monitored during these procedures. The resonance contrast remained constant during the chamber pump-down, bake-out, and atom trapping, demonstrating the robustness of the fiber-cavity mounting. However, after the chamber bake,  $\lambda_o$  was red shifted 0.11 nm from the pre-bake value and was found to increase logarithmically with exposure time to the Cs vapor as shown in Fig. 2(d).

The shift incurred during the initial bake is likely due to an accumulation on the disk surface of material desorbed from the chamber walls. Subsequent bakes did not significantly affect  $\lambda_o$ . Also, with the Cs source closed (for periods as long as 2 weeks)  $\lambda_o$  was found to remain constant. The logarithmic time dependence of  $\lambda_o$  suggests that the cesium coverage of the microdisk surface is saturating in a “glassy” manner [28]; interactions between deposited atoms quench the rate of ad-

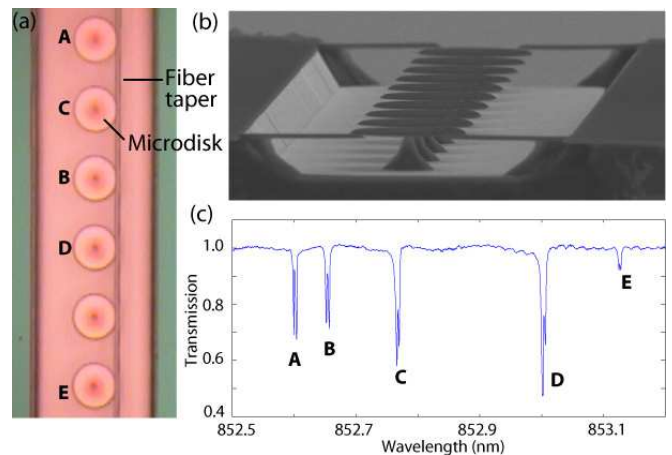


FIG. 3: (a) Top-view optical image of a fiber taper aligned with and array of 10 microdisks (the remaining 4 microdisks are out of the field of view of the image). (b) SEM image of the array of 10 microdisks. (c) Fiber taper transmission vs. wavelength when the taper is aligned with the microdisk array in (a). Letters match specific microdisks in (a) with the corresponding resonances in (c).

sorption. A shift  $\Delta\lambda_o$  of the disk resonances can be related to a surface film thickness by  $s \sim \Delta\lambda_o / (\lambda_o(n_f - 1)\Gamma')$ , where  $\Gamma'$  represents the fraction of modal energy in the film and  $n_f$  is the refractive index of the film. From finite element simulations of the microdisk,  $\Gamma' = 0.0026 \text{ nm}^{-1}$  for the  $p = 1$  TE-like mode. Assuming a film index of refraction equal to that of  $\text{SiN}_x$ , the measured wavelength shift at the longest measured time ( $t = 450 \text{ h}$ ) corresponds to roughly a half-monolayer coverage of Cs on the disk surface (monolayer thickness  $\sim 4 \text{ \AA}$  [29]).

As a future method of compensating for resonant detuning of the microdisk mode due to variation in fabrication or the time-dependent Cs surface coverage, and as an initial demonstration of the scalability of the fiber-coupled microdisk chip concept, we show in Figure 3(a) a single fiber taper coupled in parallel to an array of 10 nominally identical microdisks (Fig. 3(b)). The resulting transmission spectrum through the fiber taper is shown in Fig. 3(c). Over a 0.5 nm wavelength range the fiber taper couples to 5 of the  $p = 1$ , TE-like modes. The average spacing between modes is 0.12 nm, a gap which can be spanned by a modest  $10 \text{ }^\circ\text{C}$  of temperature tuning. Each of these resonances is due to coupling to a unique microdisk, as verified by imaging the scattered light from the microdisks during the sweep of the fiber taper transmission wavelength. Coupling to the remaining 5 disks occurred for resonant wavelengths  $\pm 1 \text{ nm}$  outside the range shown here.

In conclusion, we have shown that wavelength-scale high- $Q$  microcavities can be realized from  $\text{SiN}_x$  at near-visible wavelengths, and have demonstrated a method for integrating these devices with atom chips. The resulting optical fiber taper interface to the hybrid atom-cavity chip provides sufficient optical access for chip-based atom trapping and cooling while providing highly efficient optical coupling to single, or simul-

taneously to multiple, microdisk cavities. In the future, the use of  $\text{SiN}_x$  for the microcavity provides a path to a fully monolithic atom-cavity Si chip.

The authors thank M. Borselli and T. Johnson for assistance in FEM simulations and microdisk process development, and J. Kerckhoff for help with Cs adsorption measurements.

---

\* Electronic address: pbarclay@caltech.edu

- [1] J. Reichel, *Appl. Phys. B* **74**, 469 (2002).
- [2] R. Folman, P. Kruger, J. Schmiedmayer, J. Denschlag, and C. Henkel, *Ad. Mod. Phys.* **48**, 263 (2002).
- [3] K. J. Vahala, *Nature* **424**, 839 (2003).
- [4] B.-S. Song, S. Noda, T. Asano, and Y. Akahane, *Nat. Mat.* **4**, 207 (2005).
- [5] D. K. Armani, T. J. Kippenberg, S. M. Spillane, and K. J. Vahala, *Nature* **421**, 925 (2003).
- [6] H. J. Kimble, *Phys. Scr.*, T **T76**, 127 (1988).
- [7] L. M. Duan and H. J. Kimble, *Phys. Rev. Lett.* **12**, 127902 (2004).
- [8] P. Horak, B. G. Klappauf, A. Haase, R. Folman, J. Schmiedmayer, P. Domokos, and E. A. Hinds, *Phys. Rev. A* **67**, 043806 (2003).
- [9] B. Lev, K. Srinivasan, P. E. Barclay, O. Painter, and H. Mabuchi, *Nanotechnology* **15**, S556 (2004).
- [10] A. Haase, B. Hessmo, and J. Schmiedmayer, *Opt. Lett.* **31**, 268 (2006).
- [11] J. McKeever, A. Boca, A. D. Boozer, R. Miller, J. R. Buck, A. Kuzmich, and H. J. Kimble, *Science* **303**, 1992 (2004).
- [12] S. Groth, P. Kruger, S. Wildermuth, R. Folman, T. Fernholz, J. Schmiedmayer, D. Mahalu, and I. Bar-Joseph, *Appl. Phys. Lett.* **85**, 2980 (2004).
- [13] G. N. Parsons, J. H. Souk, and J. Batey, *J. Appl. Phys.* **70**, 1553 (1991).
- [14] T. Inukai and K. Ono, *Jpn. J. Appl. Phys.* **33**, 2593 (1994).
- [15] B. E. Little, S. T. Chu, P. P. Absil, J. V. Hryniewicz, F. Seiferth, D. Gill, V. Van. O. King, and M. Traklo, *IEEE Photonics Tech. Lett.* **16**, 2263 (2004).
- [16] T. Barwicz, M. A. Popovic, P. T. Rakich, M. R. Watts, H. A. Haus, E. P. Ippen, and H. I. Smith, *Opt. Expr.* **12**, 1437 (2004).
- [17] M. C. Netti, M. D. B. Charlton, G. J. Parker, and J. J. Baumberg, *Appl. Phys. Lett.* **76**, 991 (2000).
- [18] F. Vollmer, D. Braun, A. Libchaber, M. Khoshima, I. Teraoka, and S. Arnold, *Appl. Phys. Lett.* **80**, 4057 (2002).
- [19] A. Ksendzov and Y. Lin, *Opt. Lett.* **30**, 3344 (2005).
- [20] A. Ksendzov, M. L. Homer, and A. M. Manfreda, *IEE Elec. Lett.* **40**, 63 (2004).
- [21] M. Borselli, T. J. Johnson, and O. Painter, *Opt. Expr.* **13**, 1515 (2005).
- [22] J. Knight, G. Cheung, F. Jacques, and T. Birks, *Opt. Lett.* **22**, 1129 (1997).
- [23] S. M. Spillane, T. J. Kippenberg, K. J. Vahala, K. W. Goh, E. Wilcut, and H. J. Kimble, *Phys. Rev. A* **71**, 013817 (2005).
- [24] T. J. Kippenberg, S. M. Spillane, and K. J. Vahala, *Opt. Lett.* **27**, 1669 (2002).
- [25] P. E. Barclay, K. Srinivasan, M. Borselli, and O. Painter, *Appl. Phys. Lett.* **85**, 4 (2004).
- [26] S. M. Spillane, T. J. Kippenberg, O. J. Painter, and K. J. Vahala, *Phys. Rev. Lett.* **91**, 043902 (2003).
- [27] R. I. Abraham and E. A. Cornell, *Appl. Opt.* **37**, 1762 (1998).
- [28] R. G. Palmer, D. L. Stein, E. Abrahams, and P. W. Anderson, *Phys. Rev. Lett.* **53**, 958 (1984).
- [29] M. Brause, D. Ochs, J. Günster, T. Mayer, B. Braun, V. Puchin, W. Maus-Friedrichs, and V. Kempter, *Surf. Sci.* **383**, 216 (1997).